ELSEVIER

9 February 1998

PHYSICS LETTERS A

Physics Letters A 238 (1998) 253–257

"Worm" algorithm in quantum Monte Carlo simulations

N.V. Prokof'ev, B.V. Svistunov, I.S. Tupitsyn

Russian Research Center "Kurchatov Institute", Moscow 123182, Russia

Received 10 November 1997; accepted for publication 21 November 1997
Communicated by V.M. Agranovich

Abstract

We present a novel quantum Monte Carlo scheme which allows efficient calculations of the Green function at finite temperature and the study of large disordered systems. The scheme is ergodic, works with non-zero winding numbers and in the grand canonical ensemble. The central idea is using a pair of worldline discontinuities for sampling the extended configuration space of the system which includes both closed and disconnected worldlines. The method is illustrated by simulations of pure and disordered bosonic Hubbard models in 1D. © 1998 Published by Elsevier Science B.V.

PACS: 05.30.Ch; 02.50.Ng

With the increase in computing power it is possible now to simulate physical systems which by many standards are macroscopic, thus resembling real experimental situations. Perhaps the most powerful and universal numerical method for large systems is the quantum Monte Carlo (QMC) simulation (see, e.g., Refs. [1,2]). QMC is extremely efficient in evaluating basic thermodynamic properties like, e.g., energy, or any average of operators which are present in the structure of the Hamiltonian (like density–density or current–current correlation functions), or else are diagonal in the basis set used to describe the QMC configuration space. However, calculations of the time-dependent Green function, which is probably the most informative quantity in quantum statistics, until now were virtually impossible to perform in large systems. In what follows we specify the problem and describe a new QMC scheme, called a "worm" algorithm, which completely eliminates this essential drawback. As far as we know, in large systems, it is also the only scheme based on local Metropolis-type updates [3] which works with non-zero winding numbers and in the grand canonical ensemble. Winding numbers are important for the study of superfluid properties and such topological excitations as vortices. The advantage of working in the grand canonical ensemble (more generally, with a non-integer particle number) is crucial for disordered systems. When particles are localized, standard local-update canonical-ensemble algorithms suffer from slowing down due to many one-particle minima in the effective action: probing different classes of trajectories, corresponding to different minima, requires deep under-barrier motion. The unique feature of the "worm" algorithm – the possibility of local seeding extra worldlines at any point in the space-time – allows one to solve this problem.

As a particular example consider the Hamiltonian of interacting bosons on a lattice,

PII S0375-9601(97)00957-2

$$H = -t\sum_{\langle ij\rangle} a_i^+ a_j + \sum_{ij} U_{ij} n_i n_j + \sum_i (\mu_i - \mu) n_i \,, \tag{1}$$

where a_i^+ creates a particle on site i, $n_i = a_i^+ a_i$, t is the hopping matrix element, μ is the chemical potential, μ_i is the on-site disorder uniformly distributed between -2Δ and 2Δ, and $\langle ij\rangle$ conventionally denotes nearest-neighbor sites. In the site representation the configuration space of this model consists of all trajectories $\{n_i(\tau)\}$ in imaginary time $\tau \in (0,\beta)$ (where $\beta = 1/T$), satisfying two basic conditions: (i) they are closed, i.e., $\{n_i(\tau = 0)\} = \{n_i(\tau = \beta)\}$, and (ii) for any pair of $\tau_2 > \tau_1$ the matrix element $\langle\{n_i(\tau_2)\}|e^{-H(\tau_2-\tau_1)}|\{n_i(\tau_1)\}\rangle$ is non-zero, i.e. these trajectories are generated by the evolution operator. One may then naturally describe each trajectory by specifying the initial state $|\{n_i(\tau = 0)\}\rangle$ and all the virtual transitions in time, which we will call "kinks", when the state of the system changes [4]. The number of kinks N_K in the typical trajectory contributing to the statistics scales as $L\beta/t$, and in the state-of-the-art calculations can be as large as 10^6.

Apart from the configuration space parameterization, a QMC algorithm consists of a number of rules, or updating procedures, which describe how to go from one trajectory to another, by, e.g., changing the number of kinks, their types and time positions. In existing finite-temperature QMC schemes the updating procedures deal with closed trajectories only. This restriction usually causes no problem, since most thermodynamic quantities have non-zero expectation values for such trajectories. To generate another uncorrelated contribution to the QMC statistics one has to perform $\sim N_K$ local operations to change the entire trajectory (in loop cluster methods one update may consist of many local operations [5]), but due to the self-averaging property of the thermodynamic variables this increase in the computation time is compensated by the much smaller statistical errors.

In order to calculate the Green function $\mathcal{G}(i,\tau)$, two worldline discontinuities are inserted at time slices $\tau_1 = 0$ and $\tau_2 = \tau$ (to put it differently, one extra disconnected worldline is inserted into or removed from the interval $[\tau_1,\tau_2]$) [6,7] (see also Fig. 1). By sampling different trajectories with the fixed space-time positions of discontinuities one collects statistics for only one point of the $(d+1)$-dimensional histogram

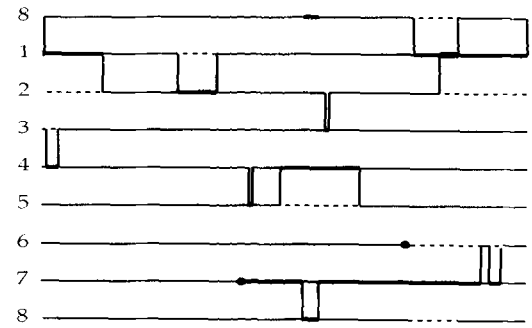

Fig. 1. A typical 8-site configuration with two worldline discontinuities (marked by filled circles). The width of the solid line is proportional to n_i, and dashed lines denote $n_i = 0$.

for $\mathcal{G}(i,\tau)$. Then the positions of the discontinuities are changed and the calculation is repeated. Thus it takes some $\sim N_K$ operations to obtain an uncorrelated contribution to the histogram, and N_K^2 operations to update the whole histogram. Note, that here self-averaging effects do not work since we are dealing with a single degree of freedom.

The so-called determinant methods [8] work differently, but with increasing system size the calculation time scales like L^3, and some of the procedures become ill-conditioned at low temperatures. Another technique allowing Green function calculations is known as Green-function Monte Carlo (or, more generally, the projection-operator) method [9]. It is applicable at zero-temperature only, and thus dynamic correlations may not be obtained by this method.

It turns out that it is possible to circumvent the above-mentioned difficulties and to construct a scheme calculating $\mathcal{G}(i,\tau)$ as efficiently as any other thermodynamic property. We call this method a "worm" algorithm, because a disconnected worldline resembles a worm. The key idea is rather simple. In the standard approach the "worm" is almost "dead"; it can change the shape but its "head" and "tail" (i.e. worldline discontinuities) are immovable. What if instead of sampling different trajectories around the dead worm, we will make it "alive" and sample different trajectories through the motion of worldline discontinuities?

In the process of motion the worm deletes existing and creates new kinks, and eventually changes the entire trajectory. Now we can even completely ignore all the other updating procedures! A typical trajectory with the worm is shown in Fig. 1. To update it we apply the following.

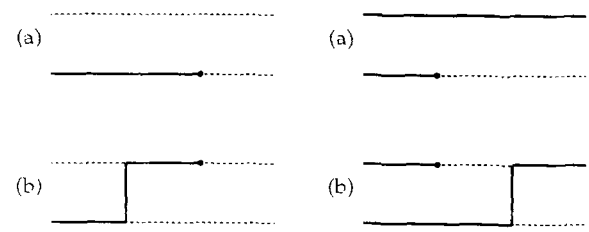

Fig. 2. Left graph: jump procedure for the discontinuity which annihilates a particle: (a) the initial trajectory, and (b) after the update. Right graph: reconnection procedure for the discontinuity annihilating a particle: (a) the initial trajectory and (b) after the update. In anti-jump and anti-reconnection (a) and (b) change places.

– *Jump/anti-jump.* This procedure is illustrated by the left graph in Fig. 2 and corresponds to the shift of the worm end in space by inserting/deleting a kink to the left of the discontinuity annihilating a particle (the "head") and to the right of the discontinuity creating a particle (the "tail").

– *Reconnection/anti-reconnection.* This procedure is illustrated by the right graph in Fig. 2 and is very close to the jump; still, we consider it separately because worldlines change places in a topologically nontrivial way; in fermionic systems any such procedure results in the change of the trajectory sign.

– *Shift in time.* This is a trivial procedure of choosing another time position for the discontinuity on an interval between the two adjacent kinks.

– *Creation and annihilation of worldline discontinuities.* The annihilation procedure deletes discontinuities and makes the trajectory closed. It can be applied, say, when the "head" and the "tail" are on the same site and there are no other kinks between them. The opposite procedure creates a short straight worm (thus seeding a new worldline, or a gap in an existing worldline).

Thus the defined updating scheme is ergodic and operates on the enlarged configuration space of the system which now includes disconnected trajectories along with the closed ones. All trajectories with non-zero winding numbers and different numbers of particles are accounted for. An extra particle is inserted/removed from the system when, e.g., the head of the worm makes a complete loop in time relative to the tail. Winding numbers are introduced by making a similar loop in space. The key advantage of this algorithm is that each local procedure adds one point to the histogram of $\mathcal{G}(i,\tau)$, except for the rare cases when there is no worm in the trajectory – these closed trajectories contribute to the statistics of standard thermodynamic variables. Hence an almost trivial idea of probing and updating trajectories through the motion of worldline discontinuities results in an incredible acceleration (up to N_K times!) of the Green function calculations.

We do not describe here how one calculates acceptance rates for the updates with worms. This is rather standard mathematics based on the so-called balance equation [1] which tells us that trajectories must contribute to the statistics according to their effective action. One may even formulate the whole scheme in continuous time [10], thus avoiding systematic errors due to artificial time discretization [11]. Formally, we notice that enlarged configuration space, which includes trajectories with the worm, corresponds to the effective action S with sources

$$S \longrightarrow S + \sum_i \int_0^\beta d\tau [\eta^* a_i(\tau) + \eta a_i^+(\tau)] ,$$

and subject to the constraint of no more than one worm in the configuration. Here η is the source strength. The details of a particular software realization of the "worm" algorithm (balance equation and updating procedures in continuous time) in our code will be published in Ref. [12]. Below we present some of the results obtained by this method which clearly demonstrate its advantages.

For Green function calculations we considered a commensurate, $\rho = 1$, 1D bosonic Hubbard model (Eq. (1) with $U_{ij} = U_0\delta_{ij}$) at the quantum critical point corresponding to the superfluid–Mott-insulator (SF–MI) phase transition of the Berezinskii–Kosterlitz–Thouless type. The parameters of the Hamiltonian at the critical point are $U_0 = 1.645\,t$ and $\mu = 1.94\,t$ (see Ref. [13]). We used the system size $L \times \beta = 450 \times 200$. In Fig. 3 we present the full-scale behavior of $\mathcal{G}(i,\tau)$ by plotting it as a function of the variable $r = \sqrt{x^2 + (c\tau)^2}$ along the time and $x = c\tau$ directions, where c is the sound velocity. In accordance with conformal invariance, for large r the two curves are indistinguishable within statistical errors. It is worth noting that for that large system these results can not be reproduced by other existing methods.

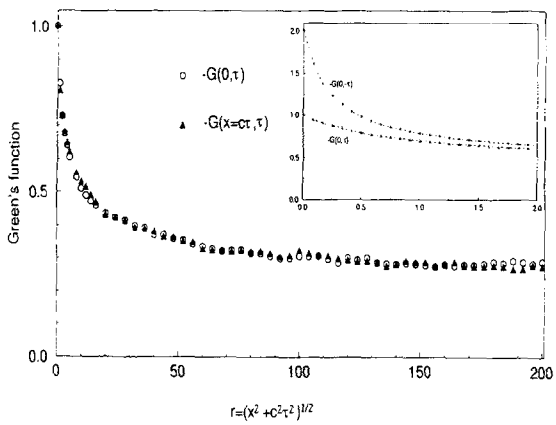

Fig. 3. Long-range behavior of $\mathcal{G}(i,\tau)$ demonstrating conformal invariance. The insert shows the short-time behavior of $\mathcal{G}$ along the τ-direction with the characteristic jump at $\tau = 0$.

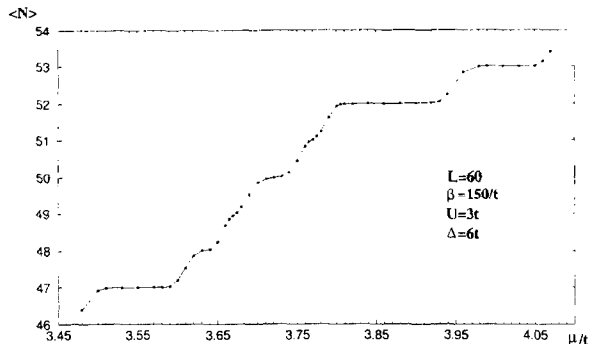

Fig. 4. Number of particles in the system versus chemical potential for the disordered Hubbard model. The calculation was done for $L = 60$ lattice sites at $\beta = 150t$; the other parameters were $U = 3t$ and $\Delta = 6t$.

The strong on-site disorder at low temperatures is a severe trial for most QMC schemes. Suppose we have the genuine ground state, $\mathcal{A}$, and a low-lying metastable state, $\mathcal{B}$, the difference between $\mathcal{A}$ and $\mathcal{B}$ being associated with just one particle, which in the metastable state is localized around some point $\boldsymbol{R}_{\mathcal{B}}$, while in the ground state it should be located around the point $\boldsymbol{R}_{\mathcal{A}}$. In a typical case the separation between the points $\boldsymbol{R}_{\mathcal{A}}$ and $\boldsymbol{R}_{\mathcal{B}}$ is on the order of the system size. It is clear that in a large system and at a sufficiently low temperature a standard worldline algorithm with local updates will fail to support a change from the class of configurations, contributing to the state $\mathcal{B}$, to the class of configurations contributing to the state $\mathcal{A}$; because of the continuity of world lines in standard algorithms, an *intermediate* configuration should contain a macroscopically large piece of worldline located in the under-barrier region. Apparently, the probability of realization of such a configuration is vanishingly small.

"Worm" algorithm naturally solves the problem by seeding an extra worldline at the point $\boldsymbol{R}_{\mathcal{A}}$ and eventually creating a new closed worldline for an extra particle around this point. In the same manner, by creating a gap in the worldline around the point $\boldsymbol{R}_{\mathcal{B}}$, one particle can be removed. No deep-under-barrier intermediate configuration is required. In Fig. 4 we plot the average particle number as a function of the chemical potential in the Bose glass (BG) phase of the Hamiltonian (1) with strong on-site disorder. The curve $\langle N\rangle(\mu)$ allows precise determination of the low-energy quasi-particle spectrum of the system with the relative accuracy of order 10^{-4}, or even better.

Finally, we apply our method to establish the ground-state phase diagram for the Hamiltonian (1). The phase boundary between the superfluid (SF) and Bose glass (BG) regions was derived from the condition $K^{-1} = \pi(\kappa\rho_s)^{1/2} = 3/2$, where κ is compressibility, and ρ_s is the superfluid stiffness in the ground state. These parameters were obtained directly from the histogram of winding and particle numbers, $W(M,N)$, which, as shown by Haldane [14], is Gaussian in the superfluid phase, $W(N,M) \propto \exp[-(L/2\beta\rho_s)M^2 - (\beta/2L\kappa)(N - \langle N\rangle)^2]$. (The critical value for the exponent K at the SF–BG transition is known [15] to be 2/3 (this was also checked via finite-size scaling analysis of ρ_s across the transition line).)

Simple considerations [16] predict the upper bound for the MI–BG transition at $\Delta = E_{\rm gap}/4$ where $E_{\rm gap}$ is the energy gap in a pure system. The corresponding line is shown in Fig. 5 by open circles utilizing the data for $E_{\rm gap}$ found in Ref. [13]. As expected [17], it is well below the SF–BG line. Precise determination of the lowest energy levels (see Fig. 4) proved that the state above the solid line at $U \simeq 2.2$ is gapless (i.e. compressible) and with an almost zero superfluid stiffness. We see that the actual phase diagram has little in common with that found in Ref. [18] by the density matrix renormalization group (DMRG) analysis, except at weak disorder where the phase boundary SF–BG was incorrectly identified with the SF–MI

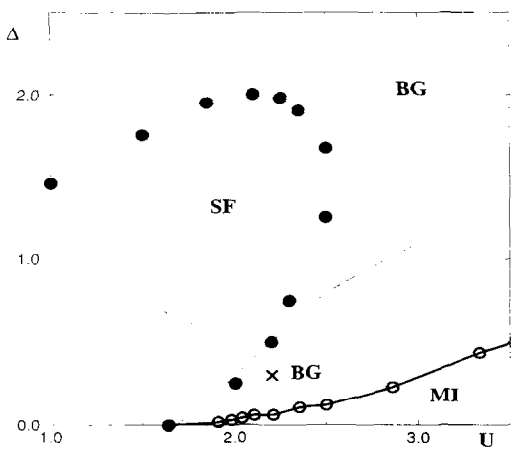

Fig. 5. The phase diagram for the Hamiltonian (1). The error bars are within the point sizes and originate mostly from the finite-size corrections (the system size used in this calculations was $L = 100$ as in Ref. [18]). The BG phase at the point marked by the cross was verified for the system with $L = 1000$ and $t/T = 200$. The dashed line indicates the results obtained by the DMRG method [18].

transition. This discrepancy originates from too small a number of basis states kept for constructing the density matrix; according to Ref. [19] a reasonable description of the disordered system with $L = 60$ by the DMRG method requires up to 750 states, while in Ref. [18] it was only 64 for $L = 100$.

The idea of considering sources as dynamic variables, which are then used to organize an efficient sampling of the system configuration space was described here for the worldline method. It is known that in systems with large correlation lengths standard worldline methods face the problem of critical slowing down (see, e.g., Refs. [5,1]). At present it is not clear to which extent the same problem appears in the "worm" algorithm. Obviously the idea may be further elaborated to consider different types of sources or more than one worm at once, e.g., in systems with pairing interactions.

We are grateful to V. Kashurnikov, A. Sandvik, M. Troyer, H. Evertz, and B. Beard for valuable discussions. This work was supported by NWO (Project No. NWO-047-003.036), and, partially, by the Russian Foundation for Basic Research (Grant No. 95-02-06191a).

References

[1] M. Suzuki, ed., Quantum Monte Carlo Methods in Condensed Matter Physics (World Scientific, Singapore, 1994).
[2] A.W. Sandvik, Proc. of the El Escorial Summer School on Strongly Correlated Magnetic and Superconducting Systems (Springer, Berlin, 1996).
[3] N. Metropolis, A.W. Rosenbluth, M.N. Rosenbluth et al., J. Chem. Phys. 21 (1953) 1087.
[4] E. Farhi, S. Gutmann, Ann. Phys. (N.Y.) 213 (1992) 182.
[5] H.G. Evertz, G. Lana, M. Marcu, Phys. Rev. Lett. 70 (1993) 875;
H.G. Evertz, M. Marcu, in: Quantum Monte Carlo Methods in Condensed Matter Physics ed. M. Suzuki (World Scientific, Singapore, 1994) p. 65 N. Kawashima, J.E. Gubernatis, J. Stat. Phys. 80 (1996) 169;
B.B. Beard, U.-J. Wiese, Phys. Rev. Lett. 77 (1996) 5130.
[6] J.E. Hirsch, D.J. Scalapino, R.L. Sugar, R. Blankenbecler, Phys. Rev. Lett. 47 (1981) 1628; Phys. Rev. B 26 (1982) 5033.
[7] E.L. Pollock, D.M. Ceperley, Phys. Rev. B 36 (1987) 8343.
[8] R. Blankenbecler, D.J. Scalapino, R.L. Sugar, Phys. Rev. D 24 (1981) 2278;
J.E. Hirsch, Phys. Rev. B 28 (1983) 4059; 31 (1985) 4403;
S.R. White, D.J. Scalapino, R.L. Sugar, E.Y. Loh, J.E. Gubernatis, R.T. Scalettar, Phys. Rev. B 40 (1989) 506;
R. Preuss, W. Hanke, W. von der Linden, Phys Rev. Lett. 75 (1995) 1344.
[9] N. Travedi, D.M. Ceperley, Phys. Rev. B 41 (1990) 4552;
S. Sorella, A. Parora, M. Parrinello, E. Tosatti, Europhys. Lett. 12 (1990) 721.
[10] N.V. Prokof'ev, B.V. Svistunov, I.S. Tupitsyn, JETP Lett. 64 (1996) 911.
[11] M. Suzuki, Prog. Theor. Phys. 56 (1976) 1454;
M. Suzuki, S. Miyashita, A. Kuroda, Theor. Phys. 58 (1977) 1377.
[12] N.V. Prokof'ev, B.V. Svistunov, I.S. Tupitsyn, cond-mat/9703200.
[13] V.A. Kashurnikov, B.V. Svistunov, Phys. Rev. B 53 (1996) 11776;
V.A. Kashurnikov, A.V. Krasavin, B.V. Svistunov, JETP Lett. 64 (1996) 99.
[14] F.D.M. Haldane, Phys. Rev. Lett. 47 (1981) 1840; J. Phys. C 14 (1981) 2585.
[15] T. Giamarchi, H.J. Schultz, Europhys. Lett. 3, 1287; Phys. Rev. B 37 (1988) 325.
[16] M.P.A. Fisher, P.B. Weichman, G. Grinstein, D.S. Fisher, Phys. Rev. B 40 (1989) 546;
J.K. Freericks, H. Monien, Phys. Rev. B 53 (1996) 2691.
[17] B.V. Svistunov, Phys. Rev. B 54 (1996) 13982.
[18] R.V. Pai, R.P. Pandit, H.R. Krishnamurthy, S. Ramasesha, Phys. Rev. Lett. 76 (1996) 2937.
[19] V. Meden, P. Schmitteckert, N. Shannon, cond-mat/9706107, submitted to Phys. Rev. B.